Dopamine-stimulated dephosphorylation of connexin 36 mediates AII amacrine cell uncoupling

W. Wade Kothmann, **Stephen C. Massey**, and **John O'Brien**
Richard S. Ruiz Department of Ophthalmology & Visual Science, University of Texas Medical School at Houston, 6431 Fannin, Houston, TX, USA

Abstract

Gap junction proteins form the substrate for electrical coupling between neurons. These electrical synapses are widespread in the central nervous system and serve a variety of important functions. In the retina, connexin 36 (Cx36) gap junctions couple AII amacrine cells and are a requisite component of the high-sensitivity rod photoreceptor pathway. AII amacrine cell coupling strength is dynamically regulated by background light intensity, and uncoupling is thought to be mediated by dopamine signaling via D1-like receptors. One proposed mechanism for this uncoupling involves dopamine-stimulated phosphorylation of Cx36 at regulatory sites, mediated by protein kinase A. Here we provide evidence against this hypothesis and demonstrate a direct relationship between Cx36 phosphorylation and AII amacrine cell coupling strength. Dopamine receptor-driven uncoupling of the AII network results from protein kinase A activation of protein phosphatase 2A and subsequent dephosphorylation of Cx36. Protein phosphatase 1 activity negatively regulates this pathway. We also find that Cx36 gap junctions can exist in widely different phosphorylation states within a single neuron, implying that coupling is controlled at the level of individual gap junctions by locally assembled signaling complexes. This kind of synapse-by-synapse plasticity allows for precise control of neuronal coupling, as well as cell type-specific responses dependent on the identity of the signaling complexes assembled.

Keywords

Connexin 36 (Cx36); Electrical Synapses; Phosphorylation; Cell-Cell Coupling; Retina; Dopamine; Phosphatase

Introduction

Electrical synapses formed by gap junctions between neurons underlie a number of important neural functions, including neuronal synchronization (Deans et al., 2001), signal averaging (DeVries et al., 2002), and network oscillations (Hormuzdi et al., 2001; Buhl et al., 2003), in addition to providing an alternative form of synaptic connection with properties that differ distinctly from the more common chemical synapses. Connexin 36 (Cx36) is the most widely expressed gap junction protein in neurons (Connors, 2009), but little is known about how intercellular coupling mediated by Cx36 is regulated. Loss of Cx36 eliminates electrical coupling and coordinated output in certain cortical interneurons (Deans et al., 2001), impairs gamma frequency oscillations in hippocampus (Hormuzdi et al., 2001; Buhl et al., 2003), causes deficits in cerebellar motor learning (Van Der Giessen et al., 2008), and eliminates the high-gain rod photoreceptor pathway (Guldenagel et al., 2001; Deans et al., 2002; Volgyi et

Correspondence should be addressed to Wade Kothmann, University of Texas Medical School at Houston, 6431 Fannin, Houston, TX, USA. Wade.Kothmann@gmail.com.

al., 2004). Cx36 is also the dominant connexin in pancreatic beta cells (Serre-Beinier et al., 2008), and loss of these gap junctions causes insulin secretion abnormalities that resemble those observed in type 2 diabetes (Wellershaus et al., 2008). Thus, understanding the regulation of Cx36 channel function is of critical importance to understanding brain and sensory system function as well as endocrine function.

The retina is an ideal tissue for studying regulation of gap junction-mediated coupling; every class of retinal neuron expresses gap junction proteins (Bloomfield and Volgyi, 2009), and the tissue remains physiologically intact when isolated from the eye. In mammalian retina the AII amacrine cell, which receives input from rod bipolar cells (Strettoi et al., 1990) and is critical for rod-mediated vision (Guldenagel et al., 2001; Deans et al., 2002; Volgyi et al., 2004), is a well-established model for studying Cx36-mediated coupling (Famiglietti and Kolb, 1975; Mills and Massey, 1995; Feigenspan et al., 2001; Mills et al., 2001; Veruki and Hartveit, 2002; Xia and Mills, 2004; Veruki et al., 2008). AII amacrine cells are extensively coupled to each other by Cx36 gap junctions under scotopic background light and are uncoupled in response to photopic background light (Bloomfield et al., 1997; Bloomfield and Volgyi, 2004), dopamine D1-like receptor (D1R) activation (Hampson et al., 1992), and protein kinase A (PKA) activation (Mills and Massey, 1995; Urschel et al., 2006). Studies in cell cultures have identified two phosphorylation sites on the fish homologue of Cx36, Ser110 and Ser276 (Ser293 in mammals), that are required for regulation of Cx36-mediated coupling by PKA (Ouyang et al., 2005). These sites have been shown to undergo dynamic changes in phosphorylation state in the retina (Kothmann et al., 2007). We therefore sought to determine the relationship between Cx36 phosphorylation and regulation of Cx36-mediated coupling by utilizing the well-described AII amacrine cell system.

Materials and Methods

Intracellular injection

Care and use of experimental animals was performed in accordance with institutional guidelines at the University of Texas Health Science Center at Houston. All experiments were performed on light-adapted animals in the daytime phase of their light cycle. Adult rabbits were anesthetized with urethane (1.5 g/kg, i.p.), and the eyes removed into Ames medium bubbled with 95% O_2/5% CO_2. Following this, the animals were killed by intracardial injection with an overdose of urethane. The superior portion of the retina was separated into several retina-sclera pieces, which were then incubated with DAPI (4,6-diamino-2-phenylindole; Molecular Probes; Eugene, OR) for 20 minutes to label cell nuclei (this short incubation labels AII amacrine cells preferentially (Mills and Massey, 1991)). Immediately before each piece was to be injected, the retina was isolated and mounted photoreceptor-side down on black nitrocellulose filters. Neurobiotin (3.5%; Vector Laboratories; Burlingame, CA) was injected by iontophoresis (±1 nA, 3 Hz) into AII amacrine cells, as described previously in detail (Xia and Mills, 2004), except that Alexa 488-conjugated biocytin (Molecular Probes) was used to visualize the microelectrode. Injections were performed for 5 minutes on an Olympus BX51WI microscope; this was followed by a 15 minute diffusion period. Each piece was superfused, starting 15 minutes prior to the start of the injection and on through the diffusion period, with either bubbled Ames medium (at 35°C) or Ames medium containing D1R agonist (SKF38393, 10 or 100 µM) or antagonist (SCH23390, 10 or 100 µM). After tracer injection and diffusion periods, the pieces of retina were fixed for 15 minutes in 4% formaldehyde in 0.1 M phosphate buffer, and subsequently immunolabeled for Cx36 and phospho-Ser293-Cx36 (Kothmann et al., 2007). Dopaminergic drugs were purchased from Tocris (Ellisville, MO).

Pharmacology experiments

Rabbit eyecups with the vitreous removed were separated into superior and inferior portions by chopping along the myelinated band with a razor blade. The central portion of the superior part from a single eye was then further separated into 4 adjacent retina-sclera pieces. Each retina-sclera piece was incubated for 20 minutes in bubbled Ames medium (at 35°C) with the appropriate pharmacologic agent. Thus, each experiment yielded one control piece and three matched pieces subjected to various pharmacological treatments. Following the incubation period, the retina-sclera pieces were fixed for 15 minutes in 4% formaldehyde in 0.1 M phosphate buffer, after which the retina was isolated, mounted photoreceptor-side down on nitrocellulose filters, and immunolabeled for Cx36 and phospho-Ser293-Cx36. The cAMP analogs were purchased from Axxora (San Diego, CA) the microcystin-LR from Calbiochem (San Diego, CA), and the tautomycetin from Tocris.

Immunolabeling

Isolated retina pieces (photoreceptor-side down on nitrocellulose filters) were first blocked overnight at 10°C in immunolabeling buffer (phosphate buffered saline with 0.5% Triton X-100, 0.1% NaN_3, pH 7.4) with 10% normal donkey serum (Jackson Immunoresearch; West Valley, PA). Pieces were then labeled with monoclonal mouse anti-Cx36 (mCx36, 1:1,000 dilution; Chemicon; Temecula, CA) and rabbit anti-phospho-Ser293-Cx36 (Ser293-P, 1:1,000 dilution) (Kothmann et al., 2007) antibodies in immunolabeling buffer with 10% donkey serum for 5 days at 10°C. Retina pieces from pharmacology experiments were also labeled with goat anti-calretinin antibodies (1:5,000 dilution; Chemicon) to label AII amacrine cells. After extensive washing, retina pieces were labeled with secondary antibodies (1:500 dilutions) in immunolabeling buffer with 5% donkey serum overnight at 10°C. For retina pieces from injection experiments, anti-calretinin labeling was replaced with Alexa 488-conjugated streptavidin (1:250 dilution) to label Neurobiotin in the injected network. Alexa 488-conjugated streptavidin and secondary antibodies were purchased from Molecular Probes. All other secondary antibodies were Cy3- or Cy5-conjugated (Jackson). Retina pieces were whole-mounted on slides with Vectashield (Vector).

Imaging and data quantification

Images were collected on a Zeiss LSM 510 Meta confocal microscope using a 63x (1.4 N.A.) or 40x (1.3 N.A.) oil immersion objectives. Imaging settings in the LSM software were identical where comparisons are made. Coupling between AII amacrine cells was quantified as the diffusion coefficient for Neurobiotin tracer transfer using a 2-dimensional compartmental diffusion model (Xia and Mills, 2004). Cx36 phosphorylation was quantified as the ratio of the mean intensity of Ser293-P to mCx36 immunofluorescence at individual regions of interest (ROIs), each identified by the mCx36 label as a single Cx36 gap junction plaque. ROI identification was accomplished using SimplePCI software (Compix; Sewickley, PA) to analyze single optical sections. ROI borders were defined by a 20% intensity threshold in the mCx36 channel and a size threshold of 0.15 μm^2. For the pharmacology experiments, an additional, empirically determined intensity threshold was added in the calretinin channel to include only the Cx36 gap junctions localized on the AII network. In our hands, this represents 96% of the Cx36 gap junctions in stratum 5 of the rabbit inner plexiform layer, in good agreement with a previously reported value of 98% (Mills et al., 2001). In the case of injected AII networks, single optical sections were collected focused on the distal dendrites of the injected cell, and all gap junctions in the field of view were included. Since 96–98% of the gap junctions at this focus depth in the retina are on AIIs, even when Neurobiotin diffusion was weak there was a very low probability of including Cx36 plaques that were not on AII amacrine cells.

In the pharmacology experiments, six images were collected at mid-peripheral eccentricity from each condition; in the injection experiments, three images were collected on different sides of each injected cell. The ratio of the mean intensity of Ser293-P to mCx36 immunofluorescence was calculated for each ROI and averaged across all ROIs in all images per condition. In this way, we collapsed the phosphorylation data into one value per condition per animal in order to perform statistical analysis.

In order to calculate the fraction of Cx36 plaques that showed any detectable phospho-Ser293 antibody labeling, regardless of its intensity, we first measured the background labeling in the Ser293-P channel for all images (measured in areas where no mCx36 labeling existed). We then set a threshold for detectable labeling at 200% of the mean background value (this value approximated the mean + 2 s.d. of the background levels observed in the initial experiments). Any Cx36 gap junction plaque with Ser293-P labeling above this threshold was considered "detectably phosphorylated" for purposes of calculating the fraction of plaques showing phosphorylation.

Images presented in the figures were collected using identical settings in the LSM software. Processing was limited to application of a 10% intensity threshold in all channels to minimize background noise.

Statistical analysis

A linear regression was used to find the correlation between relative Cx36 phosphorylation and AII amacrine cell coupling. Unpaired, two-tailed t-tests were used to compare each drug-treated condition with the control condition from the same animal. Unpaired, two-tailed t-tests were also used to compare two drug-treated conditions that shared one common drug (such as D1R agonist condition vs. D1R agonist plus phosphatase inhibitor).

Results

AII amacrine cell uncoupling is associated with dephosphorylation of Cx36

We combined intracellular injection of the Cx36-permeant tracer Neurobiotin with immunolabeling for phospho-Ser293-Cx36 in order to measure AII amacrine cell coupling and Cx36 phosphorylation in isolated rabbit retina. As previously reported (Hampson et al., 1992), AII-AII coupling was modulated by dopamine signaling (Fig.1, A–C). Activation of D1Rs (SKF38393, 10 μM) reduced AII-AII coupling (Fig. 1B), while antagonism of D1Rs (SCH23390, 100 μM) increased coupling (Fig. 1C). Phosphorylation of Cx36 at Ser293 (Ser293-P) was assessed at gap junctions on the injected AII amacrine cell dendrites and those nearby (Fig. 1, D–F; see Methods). Ser293-P was decreased by D1R activation (Fig. 1H) relative to control (Fig. 1G). Consistent with this, D1R antagonism increased Ser293-P (Fig. 1I). In order to quantify AII amacrine cell coupling, we used a compartmental diffusion model to estimate the diffusion coefficient of the Neurobiotin tracer (Xia and Mills, 2004). We quantified Ser293-P as a ratio of the mean fluorescence intensity of the phospho-Ser293-Cx36 antibody to the mean fluorescence intensity of a monoclonal Cx36 antibody at each individual gap junction plaque (for full details see Methods section). We collected three images focused on the dendrites of each injected AII amacrine cell, calculated the mean Ser293-P for all Cx36 plaques detected across all three images, and plotted this against the diffusion coefficient for Neurobiotin tracer transfer measured for that AII amacrine network (Fig. 1J). A strong correlation ($r^2 = 0.86$) was found between AII amacrine cell coupling and Cx36 phosphorylation at Ser293. Since Ser293 is known to regulate coupling through Cx36 gap junctions (Ouyang et al., 2005), this finding leads us to conclude that phosphorylation at this site increases coupling.

D1R-stimulated dephosphorylation of Cx36 is mediated by PKA

The canonical D1R signaling pathway involves a Gs-protein that activates adenylyl cyclase, thereby elevating $[cAMP]_i$ to activate PKA (Neve et al., 2004). We therefore examined the role of PKA activity in controlling Cx36 phosphorylation state downstream of D1R signaling using retina-sclera preparations (Fig. 2; see Methods). D1R activation (SKF38393, 100 µM) caused a 3.5-fold reduction in Ser293-P intensity (Fig. 2D). Inhibition of PKA (Rp-8-CPT-cAMPS, 20 µM) significantly suppressed the effect of D1R activation (Fig. 2F), resulting in intermediate Cx36 phosphorylation that was below control levels but above the levels seen with D1R activation alone. D1R antagonism (SCH23390, 100 µM) caused a 2-fold increase in Cx36 phosphorylation (Fig. 2H). As a second measure of the effects of these treatments, we determined if they altered the fraction of Cx36 plaques that showed detectable Ser293-P labeling, regardless of fluorescence intensity. Detectable Ser293-P labeling was defined as 200% of the background fluorescence in that channel (see Methods); this equated approximately to a 5% threshold in the Ser293-P channel. This measure yielded results consistent with the mean Ser293-P measurements (Fig. 2J). Histograms of the ratio of Ser293-P to mCx36 fluorescence from one representative experiment showed that D1R activation caused a leftward-shift (reduction in Ser293-P) in the population of Cx36 plaques which was blocked by inhibition of PKA, while D1R antagonism caused a rightward-shift (increase in Ser293-P) in the Cx36 population (Fig. S1). These results lead us to conclude that activation of PKA is a component of the pathway regulating Cx36-mediated coupling of AII amacrine cells. However, these results are not consistent with direct phosphorylation of Ser293 by PKA, since inhibition of this kinase led to a net increase in Cx36 phosphorylation.

We also tested the effects of dopamine itself on Cx36 phosphorylation at Ser293 in AII amacrine cells. Consistent with the effects of D1R agonist, dopamine application (1 µM) caused a 4-fold reduction in Ser293-P intensity (control, mean ratio 0.41 ± 0.06 s.e.m.; dopamine, mean ratio 0.096 ± 0.02 s.e.m.; n = 4, $p < 0.01$), as well as a similar reduction in the percentage of Cx36 plaques that showed detectable Ser293-P labeling (control, mean $69 \pm 6\%$; dopamine, mean $19 \pm 8\%$; n = 4, $p < 0.01$) (Fig. S2). This concentration of dopamine represents the upper end of estimates of the physiological extracellular dopamine concentration in the vertebrate retina (Witkovsky et al., 1993), and is known to strongly uncouple AII amacrine cells (Hampson et al., 1992;Mills and Massey, 1995). Thus, endogenous levels of dopamine should be sufficient to drive dephosphorylation of Cx36.

Modulation of Cx36 phosphorylation at Ser293 could alter coupling between AII amacrine cells in several ways. It could modulate the permeability of Cx36 gap junctions to the Neurobiotin tracer, stimulate insertion or removal of gap junction proteins from the plasma membrane at each Cx36 plaque, or cause changes in the number of gap junction plaques between AII amacrine cells. Changes in Ser293-P caused by D1R receptor activation (SKF38393, 100 µM) or antagonism (SCH23390, 100 µM) had no effect on the mean plaque size of Cx36 gap junctions or the mean number of plaques on AII dendrites in a given area (Fig. 3). Thus, the changes in tracer coupling between AII amacrine cells presented above cannot be attributed to changes in the trafficking of Cx36 proteins or the number of Cx36 gap junctions connecting AII amacrine cells. Rather, it appears that phosphorylation of Ser293 must modulate the permeability of Cx36 to the Neurobiotin tracer.

PP2A is required for D1R-stimulated dephosphorylation of Cx36

Because D1R activation reduced Ser293-P, we hypothesized that dopamine signaling increases overall phosphatase activity at Cx36 gap junctions in AII amacrine cells. In eukaryotic cells protein phosphatase 1 (PP1) and protein phosphatase 2A (PP2A) are the most abundant phosphatases (Virshup and Shenolikar, 2009); thus, we initially targeted these proteins as potential effectors of D1R-stimulated dephosphorylation of Cx36. We tested the ability of D1R

agonist to reduce Ser293-P in the presence of different phosphatase inhibitors at concentrations that preferentially inhibit either PP1 or PP2A. Microcystin-LR (0.5 nM), an inhibitor with higher affinity for PP2A (IC_{50} = 40 pM) than for PP1 (IC_{50} = 1.7 nM) (Honkanen et al., 1990), completely blocked the reduction of Ser293-P caused by D1R activation (SKF38393, 10 μM) (Fig. 4F). Application of microcystin-LR alone significantly increased Ser293-P levels relative to control (Fig. 4H), similar to the effect of D1R antagonist application. Contrasting these results, tautomycetin (10 nM), an inhibitor with higher affinity for PP1 (IC_{50} = 1.6 nM) than for PP2A (IC_{50} = 62 nM) (Mitsuhashi et al., 2001), did not prevent the D1R-mediated reduction of Ser293-P (Fig. 5F). Interestingly, inhibition of PP1 with tautomycetin in the absence of D1R activation was sufficient to cause a robust reduction in Ser293-P (Fig. 5H). As shown in the previous experiments, the percentage of Cx36 plaques showing detectable Ser293-P labeling followed the same pattern revealed by measuring the mean Ser293-P for both PP2A and PP1 inhibitors (Fig. 4J and Fig. 5J). These results provide a measure of confidence that the concentrations of microcystin-LR and tautomycetin used were selective for PP2A and PP1, respectively, as only microcystin-LR was able to block the effects of D1R activation, and since they had opposite effects on Cx36 phosphorylation when applied alone. Together, these experiments argue that PP2A is a necessary component of the D1R pathway regulating Cx36 phosphorylation and coupling strength between AII amacrine cells, and these results are consistent with direct dephosphorylation of Ser293 by PP2A. These experiments also provide evidence that PP1 is involved in regulating Cx36-mediated coupling of AII amacrine cells. However, these results are not consistent with PP1 acting directly on Ser293. Rather, they indicate that PP1 negatively regulates the pathway leading to dephosphorylation of Ser293, although the exact mechanism for this action is unclear.

PKA drives PP2A-mediated dephosphorylation of Cx36

Based on the results showing that both PKA and PP2A are downstream of D1R activation, we next asked if PP2A itself is activated by PKA in AII amacrine cells. Such a pathway has recently been described in medium-sized, spiny neurons in the striatum, where D1R-stimulated activation of PKA causes phosphorylation of the regulatory subunit of PP2A and thus increases the activity of the phosphatase (Ahn et al., 2007). These striatal neurons bear certain similarities to AII amacrine cells (namely, D1R and DARPP-32 expression) (Partida et al., 2004; Svenningsson et al., 2004; Witkovsky et al., 2007). In order to test this hypothesis, we bypassed D1Rs and directly stimulated PKA. PKA activation (Sp-8-CPT-cAMPS, 20 μM) strongly reduced mean Ser293-P in AII amacrine cells (Fig. 6D), just as D1R activation did. Inhibition of PP2A (microcystin-LR, 0.5 nM) completely blocked the PKA-mediated reduction in Ser293-P (Fig. 6F). Inhibition of PP2A alone caused a trend toward increased phosphorylation of Ser293-P (Fig. 6I), similar to the to the significant increase noted above (Fig. 4). As before, the percentage of Cx36 plaques showing detectable phospho-antibody labeling followed the same pattern established by measuring the mean Ser293-P intensity (Fig. 6J). These results confirm that PP2A is required for PKA-dependent dephosphorylation of Cx36 in AII amacrine cells, and support the existence of the D1R → PKA → PP2A pathway in these neurons.

Phosphorylation of Cx36 is controlled independently at each gap junction plaque

We frequently observed that Cx36 gap junctions in close proximity of each other existed in very different phosphorylation states, even across gap junctions positioned along a single dendrite. This was most apparent in control conditions (Fig. 2A & B, arrowheads; also Fig. S1 D). Pharmacologic activation of D1Rs reduced the heterogeneity observed in Ser293-P by causing a strong reduction in the relative degree of phosphorylation at each Cx36 plaque. Conversely, antagonism of D1Rs led to an increase in the relative degree of phosphorylation at each Cx36 plaque, indicating that dopamine-driven dephosphorylation of Cx36 is opposed by an unknown process. Thus, it appears that our control condition represents a near-equilibrium point, where conditions at some gap junction plaques favor phosphorylation of

Cx36 and conditions at others favor dephosphorylation of Cx36. The observation that this variation exists even for pairs of Cx36 plaques within a micron of one another suggests that each Cx36 gap junction plaque functions as an individual unit, the regulation of which is at least partially controlled by very local processes.

Overall, we have quantitatively demonstrated the relationship between AII amacrine cell uncoupling and Cx36 dephosphorylation. Our results describe a D1R → PKA → PP2A pathway that mediates the dephosphorylation of Cx36 at Ser293, and thus the D1R-mediated uncoupling of AII amacrine cells (Fig. 7). PP1 activity negatively regulates this dephosphorylation pathway at an unknown point. Our results indicate regulation is likely controlled at the level of individual Cx36 plaques, and that phosphorylation of Ser293 appears to influence permeability of these gap junctions, but not the trafficking of Cx36.

Discussion

One fundamental function of the retina is to adapt to fluctuating background illumination. Electrical coupling between AII amacrine cells increases the signal to noise ratio of their response to light (Vardi and Smith, 1996; Dunn et al., 2006). Modulation of coupling strength between AII amacrine cells serves to optimize signal to noise ratio for prevailing background illumination, and is one mechanism the retina uses to accomplish luminance adaptation (Bloomfield and Volgyi, 2004). In darkness AIIs are relatively uncoupled, thus preserving single-photon responses in a small group of AIIs. Coupling increases greatly under low scotopic to mesopic illumination, allowing for summation of coincident signals and improved signal to noise ratio. The AII network is uncoupled under photopic illumination by dopamine signaling. This may act to prevent contamination of cone photoreceptor signals in cone bipolar cells by saturated rod signals in AII amacrine cells. In addition, AIIs provide inhibitory glycinergic input to Off cone bipolar cells (Strettoi et al., 1992) and some Off ganglion cells (Manookin et al., 2008; Murphy and Rieke, 2008; Munch et al., 2009). Thus uncoupling of the AII network should also act to increase the spatial resolution of On cone bipolar cell-driven feed-forward inhibition of Off cone bipolar and retinal ganglion cells.

Previously it was unclear what molecular mechanism modulates coupling through Cx36 gap junctions. Although increased phosphorylation of Cx36 has been implicated as a mechanism for uncoupling gap junctions based on the dependence on PKA activity (Ouyang et al., 2005; Urschel et al., 2006), this has not been directly assessed. By making quantitative measures of tracer diffusion between AII amacrine cells and the relative phosphorylation of Cx36 gap junctions between these cells, we have determined that dephosphorylation of Ser293 is associated with uncoupling of the AII amacrine cell network. Decreases in both coupling and phosphorylation are triggered by dopamine D1R signaling and are mediated (at least in part) by activation of PKA. This finding, together with the previous finding that the Ser293 phosphorylation site is one of two that are required for regulation of Cx36 coupling by PKA activity (Ouyang et al., 2005), provides strong evidence that dephosphorylation of Cx36 at Ser293 is the mechanism by which Cx36 gap junctions are uncoupled.

It has been reported that SCH23390 (10 µM) blocks the uncoupling effect of exogenous dopamine (100 nM) application (Hampson et al., 1992). It is thus curious that in our hands 10 µM SCH23390 did not alter AII amacrine cell coupling, but 100 µM SCH23390 increased coupling. However, technical differences between our tracer coupling measurements and those made in the previous study preclude direct comparison. Hampson et al. (1992) used a more sensitive but nonlinear (peroxidise amplification) tracer detection method and 3 to 4-fold longer diffusion periods, potentially amplifying small effects. It is difficult to precisely identify the reason that a high concentration of SCH23390 was required to increase coupling in our experiments. It is possible that the non-specific binding of the drug to other targets with low-

affinity binding sites (Leonard et al., 2006; Ekelund et al., 2007) caused network effects that led to increased AII amacrine cell coupling. However, given that both the D1R agonist SKF38393 (10 µM) and dopamine (1 µM) effectively drove reductions in AII amacrine cell coupling, the specific action of SCH23390 on D1-like dopamine receptors seems most likely.

The molecular mechanism by which phosphorylation of Ser293 alters coupling through Cx36 gap junctions is still a topic for further study. We have excluded changes in the trafficking of Cx36 proteins and reduction in the absolute number of Cx36 gap junctions on AII amacrine cells as potential mechanisms by which dephosphorylation of Cx36 reduces coupling. Thus, it seems likely that dephosphorylation of Cx36 reduces its permeability to the Neurobiotin tracer. The question of what dephosphorylation of Cx36 does to the single-channel conductance and/or open probability or open duration of the channel is of more biological significance in neurons. Although our experiments here cannot directly address this measure of channel function, it has recently been shown that the junctional conductance between pairs of AII amacrine cells can change dynamically up to six-fold (Veruki et al., 2008). This increase was time-dependent and was observed with low-resistance patch pipettes, but not with high-resistance pipettes, leading the authors to suggest that the increase in coupling was due to gradual washout of an endogenous regulatory system in the AII amacrine cell. Washout of cAMP is the most prominent initial candidate, and should result in a gradual increase in the phosphorylation of Cx36.

Our results indicate that the D1R- and PKA-dependent dephosphorylation of Cx36 in AII amacrine cells requires PP2A activation. A D1R → PKA → PP2A pathway also exists in medium-sized spiny neurons of the striatum, in which Thr75 of dopamine- and cyclic-AMP-regulated phosphoprotein (DARPP-32) is one substrate for PP2A (Ahn et al., 2007). This dephosphorylation allows PKA to phosphorylate Thr34 of DARPP-32, thereby converting it into a potent inhibitor of PP1 (Svenningsson et al., 2004). DARPP-32 is also expressed by AII amacrine cells (Partida et al., 2004; Witkovsky et al., 2007), and we show that while PP1 inhibition does not mediate D1R-stimulated dephosphorylation of Cx36, PP1 inhibition alone is sufficient to cause Ser293 dephosphorylation. As PKA activation of PP2A in the striatal spiny neuron was caused by phosphorylation of the regulatory subunit of PP2A (Ahn et al., 2007), one explanation for our finding is that PP1 activity may oppose PKA-dependent activation of PP2A by phosphorylation (Fig. 7), although we did not explicitly test this hypothesis. It is clear from our results that the dopamine D1R → PKA → PP2A pathway is not limited to the striatal neurons where it was first described, but is also a component of dopamine signaling in other neurons, such as the AII amacrine cell.

In the retina, dopamine signaling originates from dopaminergic amacrine cells and is associated with light adaptation (Witkovsky, 2004). In addition to the AII amacrine cell, dopamine modulates the coupling state of other Cx36-coupled retinal neurons, such as cone photoreceptors (Lee et al., 2003; O'Brien et al., 2004; Zhang and Wu, 2004; Ribelayga et al., 2008) and OFF α ganglion cells (Hidaka et al., 2002; Mills et al., 2007). In both of these cases, however, activation of D2-like dopamine receptors triggers the uncoupling. This suggests that in cones and OFF α ganglion cells, reduced $[cAMP]_i$ and reduced PKA activity mediate uncoupling. Based on the relationship between Cx36 phosphorylation and AII amacrine coupling strength that we describe here, we would predict that in cones and OFF α ganglion cells PKA acts directly on Cx36 proteins, rather than activating a phosphatase effector, and in cones this appears to be the case (H. Li, A. Chuang, & J.O., 2009; manuscript submitted for publication). Previous reports support this possibility, as we and others have shown that PKA can directly phosphorylate regulatory residues on Cx36 *in vitro* (Ouyang et al., 2005; Urschel et al., 2006; Kothmann et al., 2007). Thus, regulation of Cx36-mediated coupling is specific to individual neuronal subtypes in the retina and is dependent on the signaling pathways they express.

The specificity of regulation that we observe in retinal neurons indicates that the signaling pathways that control coupling are likely to vary in other Cx36-coupled networks, such as those found in cortex, hippocampus, cerebellum and inferior olive, and elsewhere. For instance, several kinases converge onto the regulatory phosphorylation sites of Cx36 *in vitro*, including PKA, PKG, and CamKII (Ouyang et al., 2005; Patel et al., 2006; Urschel et al., 2006; Kothmann et al., 2007; Alev et al., 2008), suggesting that many common signaling pathways can modulate coupling. The importance of regulation of Cx36-mediated coupling in other networks is currently not well understood, as most studies have focused on the consequences of complete loss of Cx36-mediated coupling (Deans et al., 2001; Buhl et al., 2003; Van Der Giessen et al., 2008). The results we present here provide a framework for future study of coupling in these systems, where increased phosphorylation of Ser293 indicates increased coupling, and vice versa.

We commonly observed heterogeneity of Cx36 phosphorylation within individual AII amacrine cells under control conditions. This observation implies that Cx36 phosphorylation, and thus coupling, is controlled at the level of individual gap junction plaques. This possibility evokes comparisons to the postsynaptic density found at chemical synapses, where complexes of signaling proteins are assembled and provide synapse-specific modulation of important synaptic elements, such as glutamate receptors (Soderling and Derkach, 2000; Feng and Zhang, 2009). The C-terminal tail of Cx36 binds PDZ domain-containing proteins (Li et al., 2004), and may bind some of the same molecules that form the scaffolding complex at the postsynaptic density. Additionally, CamKII can bind directly to Cx36 (Alev et al., 2008), providing the means for localization of one potential regulator of coupling.

Local control of coupling would allow for the possibility of activity-dependent regulation of individual electrical synapses. This is particularly interesting to consider in the case of the AII amacrine cell, which shifts from uncoupled in dark-adapted retina to well-coupled through most of the scotopic range of vision, and which finally becomes uncoupled again under photopic visual conditions (Bloomfield and Volgyi, 2004) as a result of dopamine signaling. What causes the increase in coupling when background illumination increases from darkness to scotopic levels? One possibility is that glutamate release from rod bipolar cells causes Ca^{++} influx in the AII dendrites, leading to activation of CamKII and phosphorylation of Cx36, thus increasing coupling in a manner dependent on presynaptic activity. There are several potential sources of Ca^{++} on AII dendrites, including Ca^{++}-permeable AMPA receptors and NMDA receptors (Hartveit and Veruki, 1997; Morkve et al., 2002). One possible role for locally increasing coupling in an activity-dependent manner is to allow the spread and summation of signals from active rod bipolar cells in AII amacrine cells when photon catch is very low (near visual threshold). Gap junctions not in the vicinity of an active rod bipolar cell would remain uncoupled, and thus reduce the sharing of noisy fluctuations in the AII membrane potential. This could be particularly important in AIIs, which are inherently noisy due to the nature of the rod bipolar to AII amacrine synaptic inputs (Dunn et al., 2006). As background light intensity increases in the scotopic range, additional rod bipolar cells will become active, and continue to increase AII amacrine cell coupling, as has been described (Bloomfield and Volgyi, 2004).

Supplementary Material

Refer to Web version on PubMed Central for supplementary material.

Acknowledgments

References

Ahn JH, McAvoy T, Rakhilin SV, Nishi A, Greengard P, Nairn AC. Protein kinase A activates protein phosphatase 2A by phosphorylation of the B56delta subunit. Proc Natl Acad Sci U S A 2007;104:2979–2984. [PubMed: 17301223]

Alev C, Urschel S, Sonntag S, Zoidl G, Fort AG, Hoher T, Matsubara M, Willecke K, Spray DC, Dermietzel R. The neuronal connexin36 interacts with and is phosphorylated by CaMKII in a way similar to CaMKII interaction with glutamate receptors. Proc Natl Acad Sci U S A 2008;105:20964–20969. [PubMed: 19095792]

Bloomfield SA, Volgyi B. Function and plasticity of homologous coupling between AII amacrine cells. Vision Res 2004;44:3297–3306. [PubMed: 15535997]

Bloomfield SA, Volgyi B. The diverse functional roles and regulation of neuronal gap junctions in the retina. Nat Rev Neurosci 2009;10:495–506. [PubMed: 19491906]

Bloomfield SA, Xin D, Osborne T. Light-induced modulation of coupling between AII amacrine cells in the rabbit retina. Vis Neurosci 1997;14:565–576. [PubMed: 9194323]

Buhl DL, Harris KD, Hormuzdi SG, Monyer H, Buzsaki G. Selective impairment of hippocampal gamma oscillations in connexin-36 knock-out mouse in vivo. J Neurosci 2003;23:1013–1018. [PubMed: 12574431]

Connors, BW. Electrical signaling with neuronal gap junctions. In: Harris, AL.; Locke, D., editors. Connexins: A Guide. Humana Press; 2009. p. 143-164.

Deans MR, Gibson JR, Sellitto C, Connors BW, Paul DL. Synchronous activity of inhibitory networks in neocortex requires electrical synapses containing connexin36. Neuron 2001;31:477–485. [PubMed: 11516403]

Deans MR, Volgyi B, Goodenough DA, Bloomfield SA, Paul DL. Connexin36 is essential for transmission of rod-mediated visual signals in the mammalian retina. Neuron 2002;36:703–712. [PubMed: 12441058]

DeVries SH, Qi X, Smith R, Makous W, Sterling P. Electrical coupling between mammalian cones. Curr Biol 2002;12:1900–1907. [PubMed: 12445382]

Dunn FA, Doan T, Sampath AP, Rieke F. Controlling the gain of rod-mediated signals in the Mammalian retina. J Neurosci 2006;26:3959–3970. [PubMed: 16611812]

Ekelund J, Slifstein M, Narendran R, Guillin O, Belani H, Guo NN, Hwang Y, Hwang DR, Abi-Dargham A, Laruelle M. In vivo DA D(1) receptor selectivity of NNC 112 and SCH 23390. Mol Imaging Biol 2007;9:117–125. [PubMed: 17473957]

Famiglietti EV Jr, Kolb H. A bistratified amacrine cell and synaptic ciruicitry in the inner plexiform layer of the retina. Brain Res 1975;84:293–300. [PubMed: 1111833]

Feigenspan A, Teubner B, Willecke K, Weiler R. Expression of neuronal connexin36 in AII amacrine cells of the mammalian retina. J Neurosci 2001;21:230–239. [PubMed: 11150340]

Feng W, Zhang M. Organization and dynamics of PDZ-domain-related supramodules in the postsynaptic density. Nat Rev Neurosci 2009;10:87–99. [PubMed: 19153575]

Guldenagel M, Ammermuller J, Feigenspan A, Teubner B, Degen J, Sohl G, Willecke K, Weiler R. Visual transmission deficits in mice with targeted disruption of the gap junction gene connexin36. J Neurosci 2001;21:6036–6044. [PubMed: 11487627]

Hampson EC, Vaney DI, Weiler R. Dopaminergic modulation of gap junction permeability between amacrine cells in mammalian retina. J Neurosci 1992;12:4911–4922. [PubMed: 1281499]

Hartveit E, Veruki ML. AII amacrine cells express functional NMDA receptors. Neuroreport 1997;8:1219–1223. [PubMed: 9175117]

Hidaka S, Kato T, Miyachi E. Expression of gap junction connexin36 in adult rat retinal ganglion cells. J Integr Neurosci 2002;1:3–22. [PubMed: 15011262]

Honkanen RE, Zwiller J, Moore RE, Daily SL, Khatra BS, Dukelow M, Boynton AL. Characterization of microcystin-LR, a potent inhibitor of type 1 and type 2A protein phosphatases. J Biol Chem 1990;265:19401–19404. [PubMed: 2174036]

Hormuzdi SG, Pais I, LeBeau FE, Towers SK, Rozov A, Buhl EH, Whittington MA, Monyer H. Impaired electrical signaling disrupts gamma frequency oscillations in connexin 36-deficient mice. Neuron 2001;31:487–495. [PubMed: 11516404]

Kothmann WW, Li X, Burr GS, O'Brien J. Connexin 35/36 is phosphorylated at regulatory sites in the retina. Vis Neurosci 2007;24:363–375. [PubMed: 17640446]

Lee EJ, Han JW, Kim HJ, Kim IB, Lee MY, Oh SJ, Chung JW, Chun MH. The immunocytochemical localization of connexin 36 at rod and cone gap junctions in the guinea pig retina. Eur J Neurosci 2003;18:2925–2934. [PubMed: 14656288]

Leonard SK, Ferry-Leeper P, Mailman RB. Low affinity binding of the classical D1 antagonist SCH23390 in rodent brain: potential interaction with A2A and D2-like receptors. Brain Res 2006;1117:25–37. [PubMed: 16962565]

Li X, Olson C, Lu S, Kamasawa N, Yasumura T, Rash JE, Nagy JI. Neuronal connexin36 association with zonula occludens-1 protein (ZO-1) in mouse brain and interaction with the first PDZ domain of ZO-1. Eur J Neurosci 2004;19:2132–2146. [PubMed: 15090040]

Manookin MB, Beaudoin DL, Ernst ZR, Flagel LJ, Demb JB. Disinhibition combines with excitation to extend the operating range of the OFF visual pathway in daylight. J Neurosci 2008;28:4136–4150. [PubMed: 18417693]

Mills SL, Massey SC. Labeling and distribution of AII amacrine cells in the rabbit retina. J Comp Neurol 1991;304:491–501. [PubMed: 1850763]

Mills SL, Massey SC. Differential properties of two gap junctional pathways made by AII amacrine cells. Nature 1995;377:734–737. [PubMed: 7477263]

Mills SL, O'Brien JJ, Li W, O'Brien J, Massey SC. Rod pathways in the mammalian retina use connexin 36. J Comp Neurol 2001;436:336–350. [PubMed: 11438934]

Mills SL, Xia XB, Hoshi H, Firth SI, Rice ME, Frishman LJ, Marshak DW. Dopaminergic modulation of tracer coupling in a ganglion-amacrine cell network. Vis Neurosci 2007;24:593–608. [PubMed: 17711603]

Mitsuhashi S, Matsuura N, Ubukata M, Oikawa H, Shima H, Kikuchi K. Tautomycetin is a novel and specific inhibitor of serine/threonine protein phosphatase type 1, PP1. Biochem Biophys Res Commun 2001;287:328–331. [PubMed: 11554729]

Morkve SH, Veruki ML, Hartveit E. Functional characteristics of non-NMDA-type ionotropic glutamate receptor channels in AII amacrine cells in rat retina. J Physiol 2002;542:147–165. [PubMed: 12096058]

Munch TA, da Silveira RA, Siegert S, Viney TJ, Awatramani GB, Roska B. Approach sensitivity in the retina processed by a multifunctional neural circuit. Nat Neurosci. 2009

Murphy GJ, Rieke F. Signals and noise in an inhibitory interneuron diverge to control activity in nearby retinal ganglion cells. Nat Neurosci 2008;11:318–326. [PubMed: 18223648]

Neve KA, Seamans JK, Trantham-Davidson H. Dopamine receptor signaling. J Recept Signal Transduct Res 2004;24:165–205. [PubMed: 15521361]

O'Brien J, Nguyen HB, Mills SL. Cone photoreceptors in bass retina use two connexins to mediate electrical coupling. J Neurosci 2004;24:5632–5642. [PubMed: 15201336]

Ouyang X, Winbow VM, Patel LS, Burr GS, Mitchell CK, O'Brien J. Protein kinase A mediates regulation of gap junctions containing connexin35 through a complex pathway. Brain Res Mol Brain Res 2005;135:1–11. [PubMed: 15857663]

Partida GJ, Lee SC, Haft-Candell L, Nichols GS, Ishida AT. DARPP-32-like immunoreactivity in AII amacrine cells of rat retina. J Comp Neurol 2004;480:251–263. [PubMed: 15515184]

Patel LS, Mitchell CK, Dubinsky WP, O'Brien J. Regulation of gap junction coupling through the neuronal connexin Cx35 by nitric oxide and cGMP. Cell Commun Adhes 2006;13:41–54. [PubMed: 16613779]

Ribelayga C, Cao Y, Mangel SC. The circadian clock in the retina controls rod-cone coupling. Neuron 2008;59:790–801. [PubMed: 18786362]

Serre-Beinier V, Bosco D, Zulianello L, Charollais A, Caille D, Charpantier E, Gauthier BR, Diaferia GR, Giepmans BN, Lupi R, Marchetti P, Deng S, Buhler L, Berney T, Cirulli V, Meda P. Cx36 makes channels coupling human pancreatic {beta} - cells, and correlates with insulin expression. Hum Mol Genet. 2008

Soderling TR, Derkach VA. Postsynaptic protein phosphorylation and LTP. Trends Neurosci 2000;23:75–80. [PubMed: 10652548]

Strettoi E, Dacheux RF, Raviola E. Synaptic connections of rod bipolar cells in the inner plexiform layer of the rabbit retina. J Comp Neurol 1990;295:449–466. [PubMed: 2351763]

Strettoi E, Raviola E, Dacheux RF. Synaptic connections of the narrow-field, bistratified rod amacrine cell (AII) in the rabbit retina. J Comp Neurol 1992;325:152–168. [PubMed: 1460111]

Svenningsson P, Nishi A, Fisone G, Girault JA, Nairn AC, Greengard P. DARPP-32: an integrator of neurotransmission. Annu Rev Pharmacol Toxicol 2004;44:269–296. [PubMed: 14744247]

Urschel S, Hoher T, Schubert T, Alev C, Sohl G, Worsdorfer P, Asahara T, Dermietzel R, Weiler R, Willecke K. Protein kinase A-mediated phosphorylation of connexin36 in mouse retina results in decreased gap junctional communication between AII amacrine cells. J Biol Chem 2006;281:33163–33171. [PubMed: 16956882]

Van Der Giessen RS, Koekkoek SK, van Dorp S, De Gruijl JR, Cupido A, Khosrovani S, Dortland B, Wellershaus K, Degen J, Deuchars J, Fuchs EC, Monyer H, Willecke K, De Jeu MT, De Zeeuw CI. Role of olivary electrical coupling in cerebellar motor learning. Neuron 2008;58:599–612. [PubMed: 18498740]

Vardi N, Smith RG. The AII amacrine network: coupling can increase correlated activity. Vision Res 1996;36:3743–3757. [PubMed: 8994576]

Veruki ML, Hartveit E. AII (Rod) amacrine cells form a network of electrically coupled interneurons in the mammalian retina. Neuron 2002;33:935–946. [PubMed: 11906699]

Veruki ML, Oltedal L, Hartveit E. Electrical Synapses Between AII Amacrine Cells: Dynamic Range and Functional Consequences of Variation in Junctional Conductance. J Neurophysiol 2008;100:3305–3322. [PubMed: 18922943]

Virshup DM, Shenolikar S. From promiscuity to precision: protein phosphatases get a makeover. Mol Cell 2009;33:537–545. [PubMed: 19285938]

Volgyi B, Deans MR, Paul DL, Bloomfield SA. Convergence and segregation of the multiple rod pathways in mammalian retina. J Neurosci 2004;24:11182–11192. [PubMed: 15590935]

Wellershaus K, Degen J, Deuchars J, Theis M, Charollais A, Caille D, Gauthier B, Janssen-Bienhold U, Sonntag S, Herrera P, Meda P, Willecke K. A new conditional mouse mutant reveals specific expression and functions of connexin36 in neurons and pancreatic beta-cells. Exp Cell Res 2008;314:997–1012. [PubMed: 18258229]

Witkovsky P. Dopamine and retinal function. Doc Ophthalmol 2004;108:17–40. [PubMed: 15104164]

Witkovsky P, Nicholson C, Rice ME, Bohmaker K, Meller E. Extracellular dopamine concentration in the retina of the clawed frog, Xenopus laevis. Proc Natl Acad Sci U S A 1993;90:5667–5671. [PubMed: 8516316]

Witkovsky P, Svenningsson P, Yan L, Bateup H, Silver R. Cellular localization and function of DARPP-32 in the rodent retina. Eur J Neurosci 2007;25:3233–3242. [PubMed: 17552992]

Xia XB, Mills SL. Gap junctional regulatory mechanisms in the AII amacrine cell of the rabbit retina. Vis Neurosci 2004;21:791–805. [PubMed: 15683564]

Zhang J, Wu SM. Connexin35/36 gap junction proteins are expressed in photoreceptors of the tiger salamander retina. J Comp Neurol 2004;470:1–12. [PubMed: 14755521]
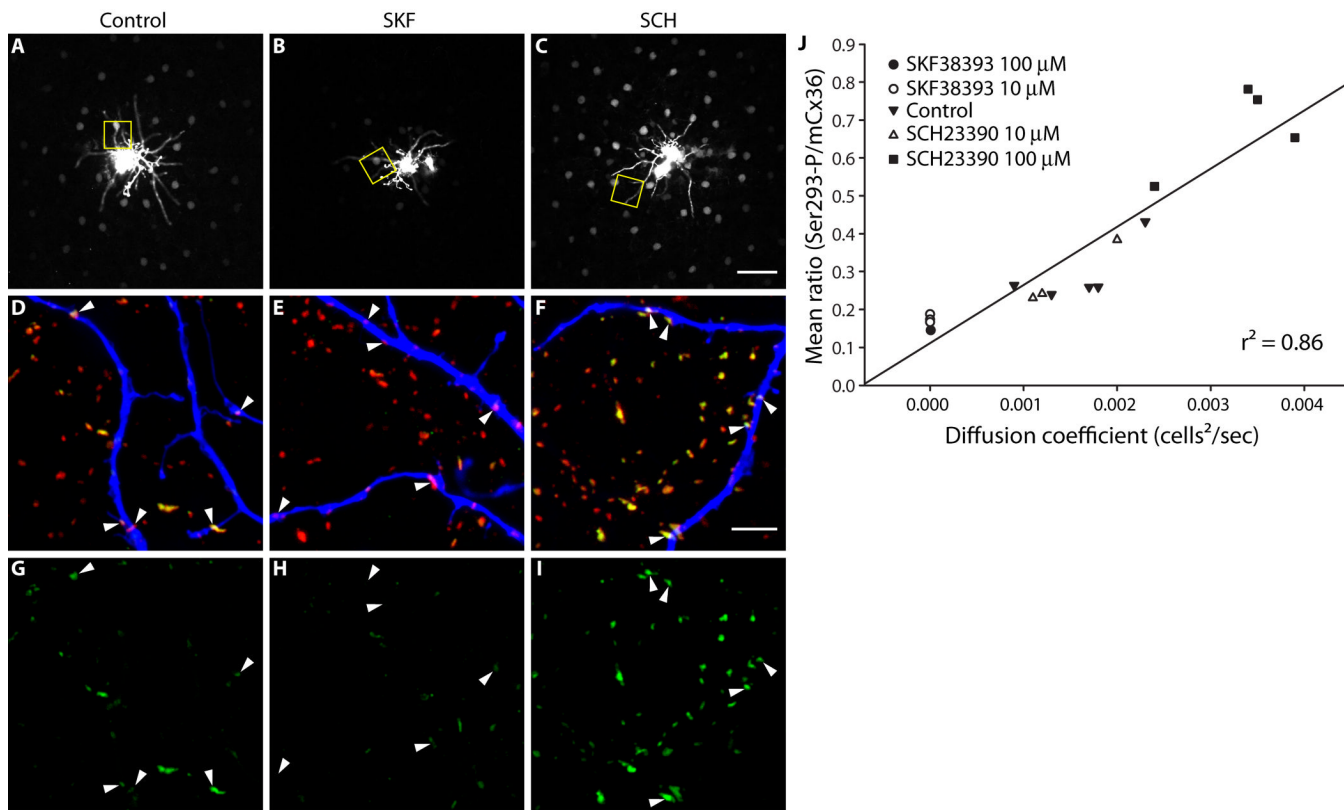
Figure 1. AII amacrine cell coupling is directly related to Cx36 phosphorylation at Ser293
A–C, Neurobiotin tracer coupling between AII amacrine cells is modulated by dopamine D1R signaling. D1R activation (**B**, SKF38393, 10 µM) reduced the extent of Neurobiotin diffusion relative to control (**A**). D1R antagonism (**C**, SCH23390, 100 µM) increased tracer diffusion. Images are mini-stacks (2 µm in z-depth) focused on the somas of the AII amacrine cells. Yellow boxes highlight areas shown in **D–I** (at different focal depth). **D–F**, Cx36 gap junctions, labeled with mCx36 antibody (red) and Ser293-P antibody (green), on and around the dendrites of the injected AII amacrine cell, labeled with fluorophore-conjugated Streptavidin (blue). The Cx36 gap junctions not on the injected cell are primarily on other AII amacrine cells (see Methods). Arrowheads identify prominent Cx36 gap junctions on the injected cells. **G–I**, Phosphorylation of Cx36 at Ser293, a site known to regulate coupling through Cx36 gap junctions (Ouyang et al., 2005), is also modulated by dopamine D1R signaling. Arrowheads identify the locations of the same Cx36 gap junctions identified in **D–F**. D1R activation (**H**, SKF38393, 10 µM) reduced Ser293-P labeling relative to control (**G**). D1R antagonism (**I**, SCH23390, 100 µM) increased Ser293-P labeling. **J**, Quantification of the relationship between AII amacrine cell coupling and Cx36 phosphorylation at Ser293. The mean ratio of Ser293-P intensity to mCx36 intensity (across all Cx36 gap junctions in 3 images per injection) is plotted against the diffusion coefficient for Neurobiotin tracer transfer calculated for each injected AII amacrine cell network. The strong correlation of the data ($r^2 = 0.86$) indicates a direct relationship between AII amacrine cell coupling and Cx36 phosphorylation at Ser293. Images are 2 µm-deep stacks. Scale bar in **C** is 50 µm; bar in **F** is 5 µm.
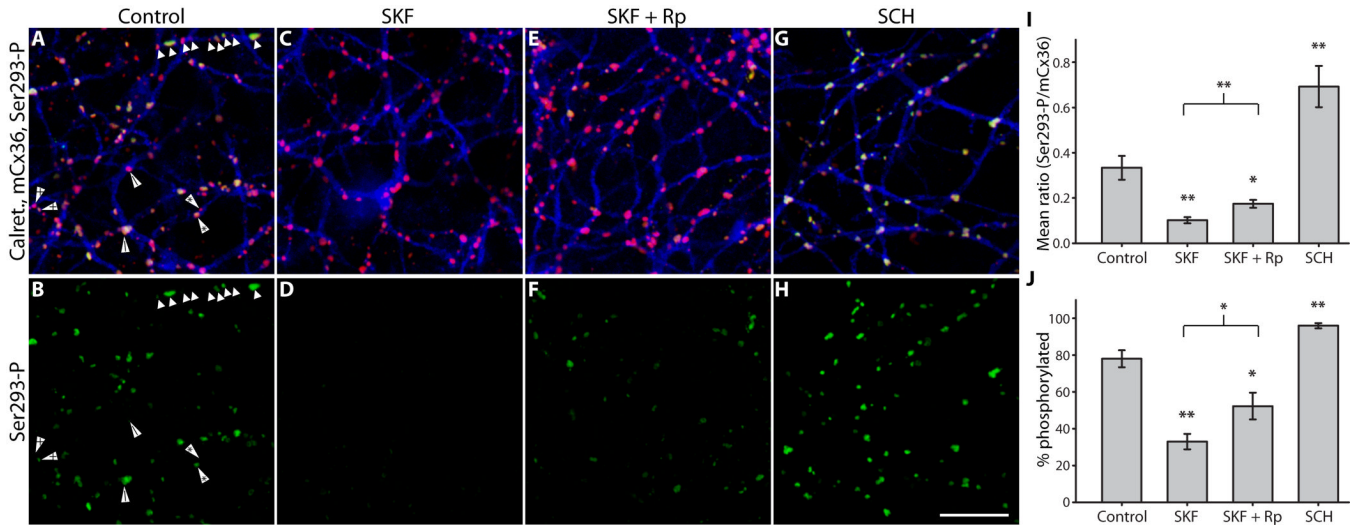
Figure 2. PKA mediates D1R-dependent dephosphorylation of Cx36 at Ser293 in AII amacrine cells

A & B, Under control conditions Ser293-P (green) labeling of Cx36 gap junctions (mCx36, red) on AII amacrine cells (calretinin, blue) was heterogeneous. Annotated arrowheads indicate pairs of Cx36 plaques along single dendrites that are in different phosphorylation states. The close proximity of Cx36 plaques with widely varying Ser293-P labeling implies that regulation is locally controlled at individual plaques. **C & D**, D1R activation (SKF38393, 100 µM) greatly diminished Ser293-P labeling. **E & F**, Inhibition of PKA (Rp-8-CPT-cAMPS, 20 µM) attenuated the dramatic reduction in Ser293-P labeling caused by SKF38393 (100 µM). **G & H**, Antagonism of D1Rs (SCH23390, 100 µM) increased Ser293-P labeling. **I**, Summary of data shows that inhibition of PKA significantly suppressed the reduction in Ser293 phosphorylation caused by D1R activation. **J**, Summary of data shows that changes in the percentage of Cx36 plaques that show detectable Ser293-P labeling follows the same pattern established for relative Ser293-P measurements in **I**. Error bars are s.e.m, n = 6. Asterisk denotes $P < 0.05$, two asterisks denote $P < 0.01$. Images are 1 µm-deep stacks. Scale bar in **H** is 10 µm.

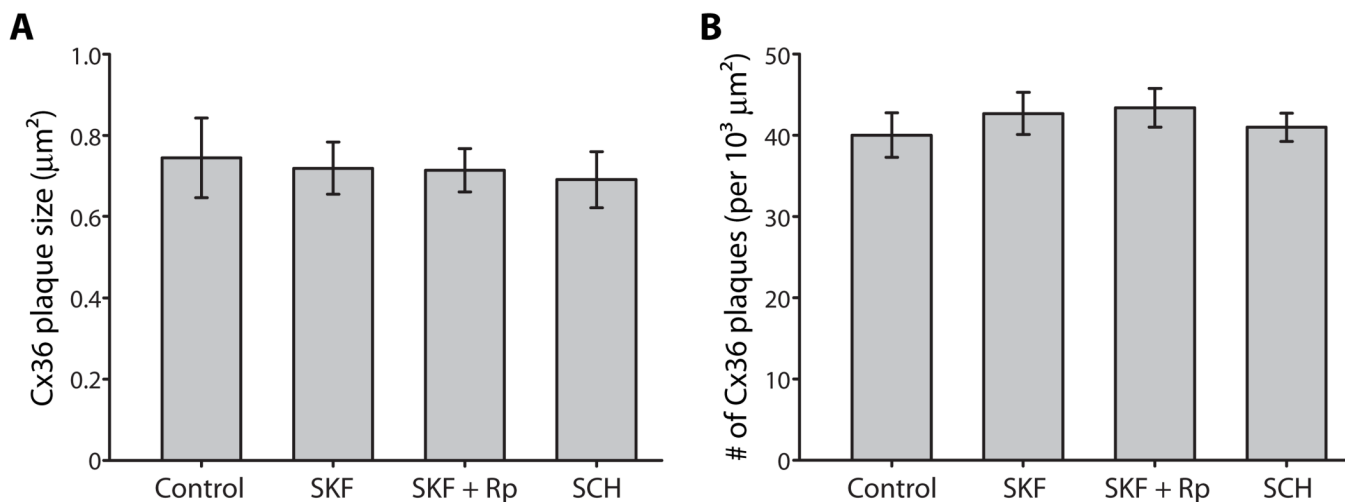**A**

B

Figure 3. Phosphorylation of Ser293 on Cx36 does not alter trafficking or distribution of the protein
A, Conditions that altered Cx36 phosphorylation at Ser293 (D1R activation, SKF38393, 100 µM; D1R antagonism, SCH23390, 100 µM) had no effect on the size of Cx36 plaques in AII amacrine cells. Inhibition of PKA (Rp-8-CPT-cAMPS, 20 µM) also had no effect on Cx36 plaque size. **B**, Conditions that altered Cx36 phosphorylation at Ser293 (D1R activation, SKF38393, 100 µM; D1R antagonism, SCH23390, 100 µM) had no effect on the overall distribution of Cx36 plaques in AII amacrine cells. Inhibition of PKA (Rp-8-CPT-cAMPS, 20 µM) also had no effect on Cx36 plaque distribution. Error bars are s.e.m, n = 5. No significant changes were found.
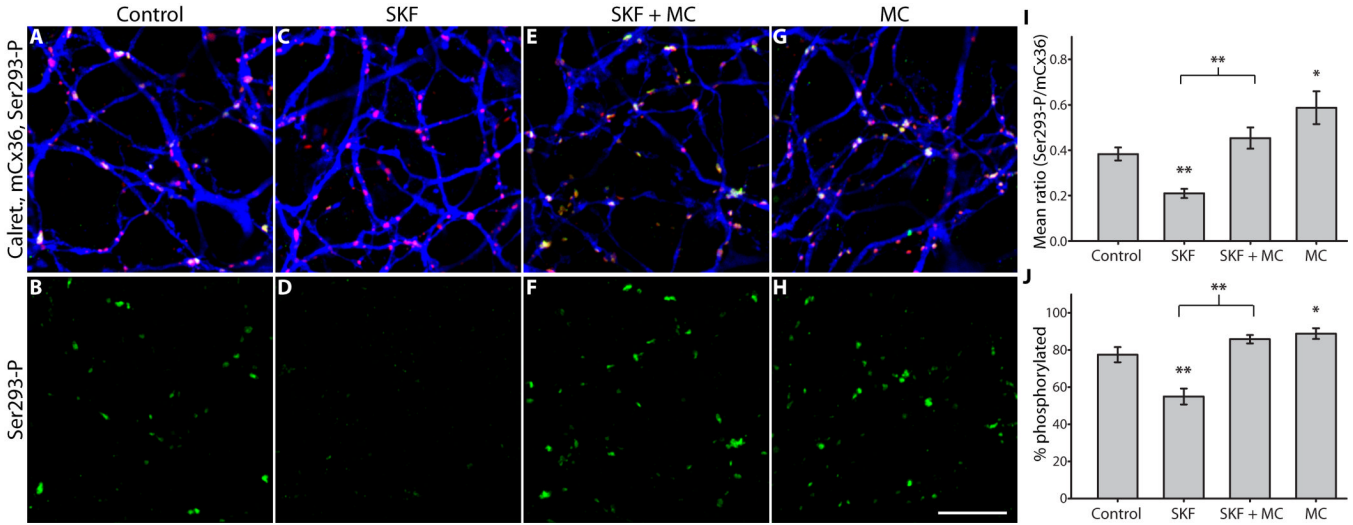
Figure 4. PP2A is required for D1R-dependent dephosphorylation of Cx36 at Ser293 in AII amacrine cells

A & B, Control; color scheme and antibodies are the same as Figure 2. **C & D**, D1R activation (SKF38393, 10 µM) greatly diminished Ser293-P labeling. **E & F**, Inhibition of PP2A (microcystin-LR, 0.5 nM) completely blocked the reduction in Ser293 phosphorylation caused by D1R activation. **G & H**, Inhibition of PP2A alone led to increased phosphorylation of Ser293. **I**, Summary of data shows that inhibition of PP2A significantly blocked the reduction in Ser293 phosphorylation caused by D1R activation, and that PP2A inhibition alone significantly increased Ser293 phosphorylation. **J**, Summary of data shows that changes in the percentage of Cx36 plaques that show detectable Ser293-P labeling follows the same pattern established for relative Ser293-P measurements in **I**. Error bars are s.e.m, n = 6. Asterisk denotes $P < 0.05$, two asterisks denote $P < 0.01$. Images are 1 µm-deep stacks. Scale bar in **H** is 10 µm.
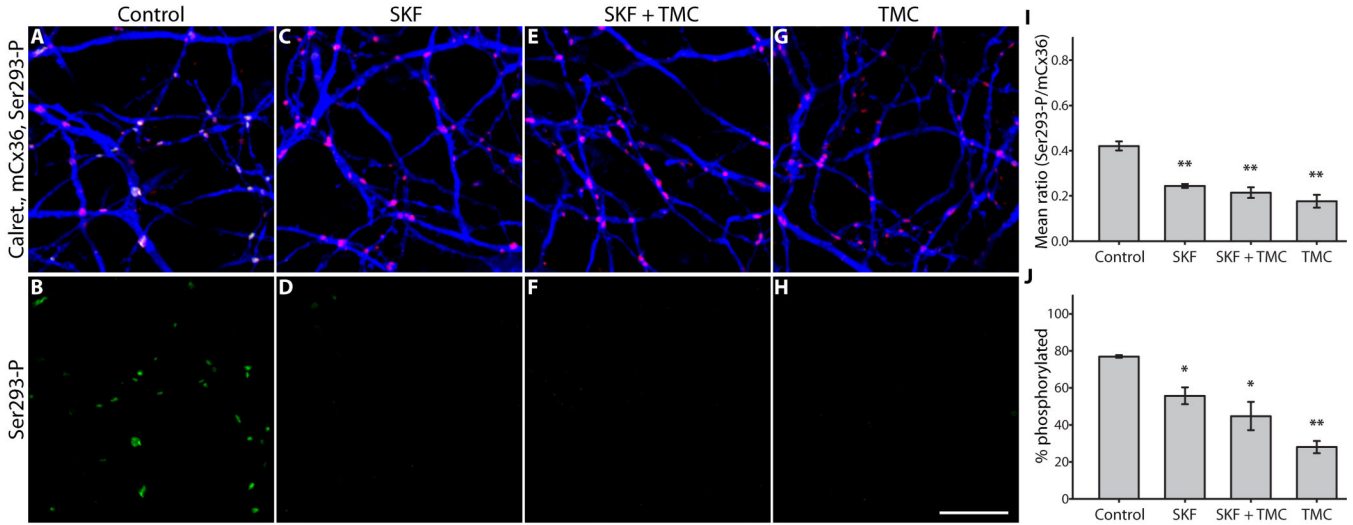
Figure 5. PP1 negatively regulates the dephosphorylation of Cx36
A & B, Control; color scheme and antibodies are the same as Figure 2. **C & D**, D1R activation (SKF38393, 10 µM) greatly diminished Ser293-P labeling. **E & F**, Inhibition of PP1 (tautomycetin, 10 nM) did not alter the effects of D1R activation. **G & H**, Inhibition of PP1 alone was sufficient to cause a strong reduction in Ser293-P labeling. **I**, Summary of data shows that inhibition of PP1 did not prevent the reduction in Ser293 phosphorylation caused by D1R activation, and that PP1 inhibition alone significantly reduced Ser293 phosphorylation. **J**, Summary of data shows that changes in the percentage of Cx36 plaques that show detectable Ser293-P labeling follows the same pattern established for relative Ser293-P measurements in **I**. Error bars are s.e.m, n = 4. Asterisk denotes $P < 0.05$, two asterisks denote $P < 0.01$. Images are 1 µm-deep stacks. Scale bar in **H** is 10 µm.
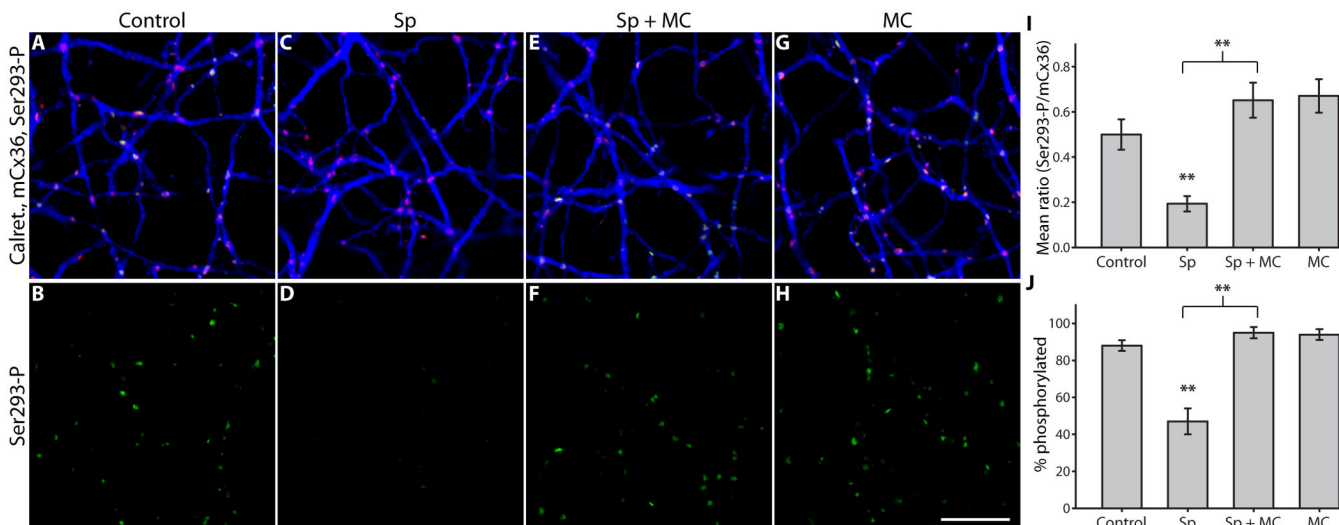
Figure 6. PP2A is required for PKA-dependent dephosphorylation of Cx36 at Ser293 in AII amacrine cells

A & B, Control; color scheme and antibodies are the same as Figure 2. **C & D**, PKA activation (Sp-8-CPT-cAMPS, 20 µM) greatly diminished Ser293-P labeling, just as D1R activation did. **E & F**, Inhibition of PP2A (microcystin-LR, 0.5 nM) completely blocked the reduction in Ser293 phosphorylation caused by PKA activation. **G & H**, Inhibition of PP2A alone slightly increased Ser293 phosphorylation relative to control. **I**, Summary of data shows that inhibition of PP2A significantly blocked the reduction in Ser293 phosphorylation caused by PKA activation. We observed a trend towards increased Ser293 phosphorylation when PP2A alone was inhibited, similar to the significant increase we observed previously with the same treatment (Fig. 4). **J**, Summary of data shows that changes in the percentage of Cx36 plaques that show detectable Ser293-P labeling follows the same pattern established for relative Ser293-P measurements in **I**. Error bars are s.e.m, n = 5. Two asterisks denote $P < 0.01$. Images are 1 µm-deep stacks. Scale bar in **H** is 10 µm.
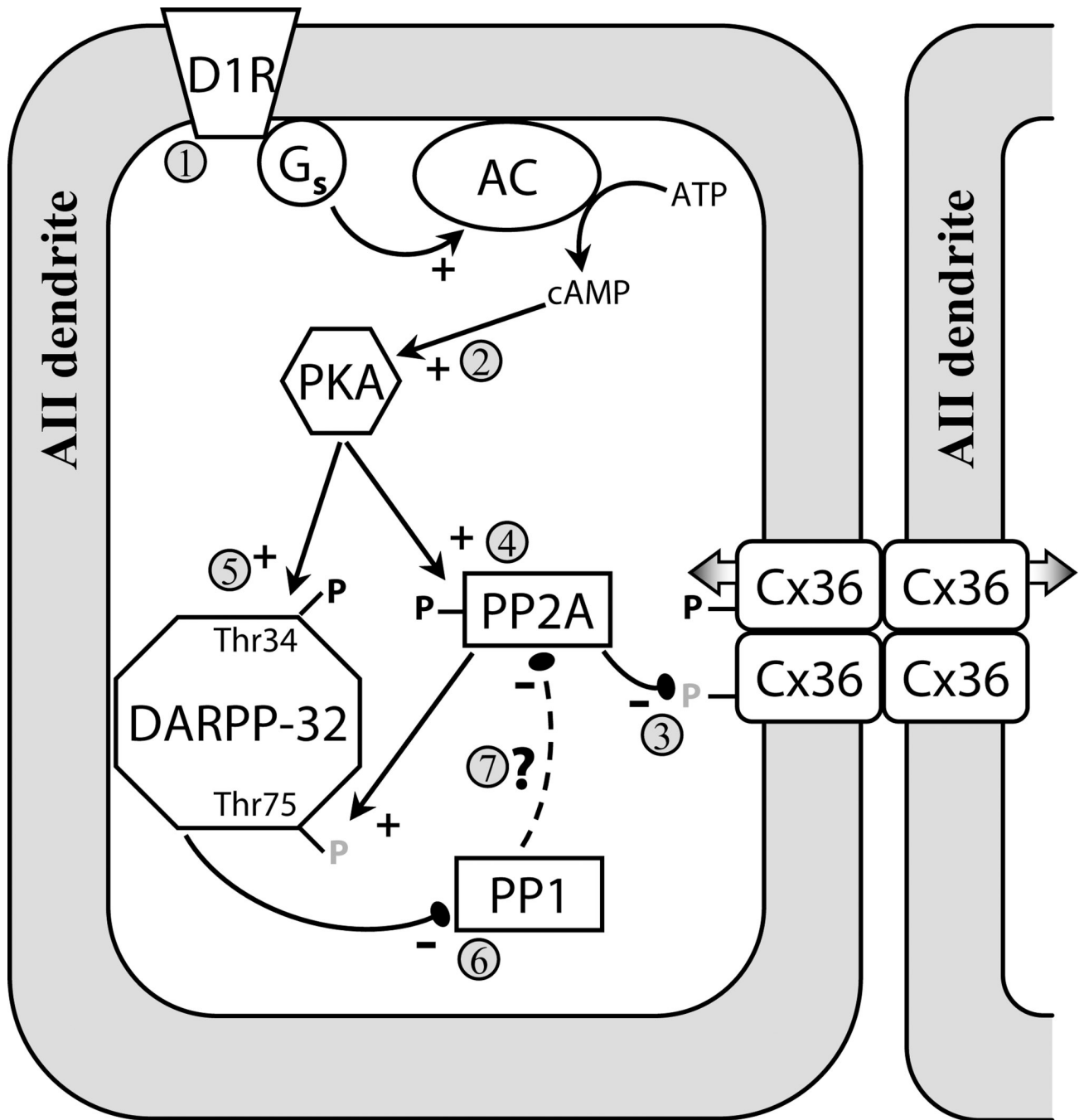
Figure 7. Model of D1R-dependent regulation of Cx36-mediated coupling between AII amacrine cells

Activation of D1Rs (1) initiates a cascade leading to activation of PKA (2); both D1R and PKA activation are sufficient to uncouple AII amacrine cells (Hampson et al., 1992; Mills and Massey, 1995). In this study we showed that D1R-dependent dephosphorylation (grey P's) of Ser293 on Cx36 uncouples AII amacrine cells (3). We show that PP2A is required for both D1R- and PKA-stimulated dephosphorylation of Ser293 (4). This provides evidence that the D1R → PKA → PP2A pathway, which was recently described in spiny neurons in the striatum and led to dephosphorylation of Thr75 on DARPP-32 (Ahn et al., 2007), is also present in the AII amacrine cell. AII amacrine cells also express DARPP-32 (Partida et al., 2004; Witkovsky

et al., 2007), and dephosphorylation of Thr75 on DARPP-32 facilitates PKA-mediated phosphorylation (black P's) of Thr34 (5), which converts DAPRR-32 into an inhibitor of PP1 (6) (Svenningsson et al., 2004). We found that PP1 negatively regulates the dephosphorylation of Cx36, possibly by opposing PKA-mediated activation of PP2A (7). Our results indicate that the D1R → PKA → PP2A pathway is not limited to striatal neurons, and may represent a common pathway in neurons expressing D1Rs and DARPP-32.